Stress-strain curve for aluminium from a continuous indentation test

W. H. ROBINSON,
Materials Science Section, Physics & Engineering Laboratory, D.S.I.R. Lower Hutt, New Zealand

S. D. TRUMAN
Department of Chemical and Materials Engineering, University of Auckland, Auckland, New Zealand

Continuous indentation tests using a 6.35 mm diameter steel ball were carried out on polycrystalline aluminium (99.995%) at forces up to 942 N (96 kg) and a total displacement of 65 μm. On loading the results were observed to follow the classical Hertz equation until the elastic limit was reached at 4.6 ± 0.2 N (0.47 kg), 1.02 ± 0.05 μm. The unloading results after plastic indentation were found to fit the Hertz solution for an indenter in a spherical hole. Using the Hertz theory it was possible from the unloading results to determine the mean stress and strain under the ball, together with the indentation diameter, plastic strain, Meyer stress and ratio of elastic to total strain, enabling a stress–strain curve for hardness to be drawn. The elastic limit of aluminium occurred at a stress of $4.7 \pm 0.2 \times 10^8$ Pa (46 kg mm^{-2}) and a strain of 1.27 ± .05%. At a total strain of 11.25% the stress was $11.7 \pm 0.2 \times 10^8$ Pa (115 kg mm^{-2}).

1. Introduction

The continuous indentation test has been used by a number of researchers to study hardness. Bunshah and Armstrong [1] measured the hardness of brass from a continuous test and expressed their results in terms of the Meyer stress. Armstrong and Robinson [2, 3] observed the elastic and plastic deformation of KCl and from their results formed a stress–strain curve (by the addition of elastic and plastic areas) which in the elastic region agreed with the Hertz solution for the mean stress under the indenter and in the plastic region approached the Meyer stress. Cousins *et al.* [4] successfully followed the elastic deformation of lignin, a component of wood, and were, from their results, able to form an elastic stress–strain curve and determine the Young's modulus of lignin. In this paper we present results for the elastic and plastic deformation of aluminium obtained at higher sensitivity (~ ±0.02 μm) than used previously and using the Hertz theory we determine a stress–strain curve for hardness together with curves for the Meyer stress, indentation diameter and ratio of elastic to total strain. These stress–strain curves differ from our previous work in that in the plastic region they were determined solely from the elastic unloading curves rather than by the less rigorous addition of elastic and plastic areas.

2. Test procedure

The test end of the 99.995% aluminium specimen (grain size < 1 μm) was polished to a mirror finish with Buehler micropolish *C* (< 1 μm) alpha alumina. The opposite end of the 20 mm diameter by 30 mm cylindrical specimen was ground flat with 400 paper. The steel ball (6.35 mm diameter) assembly was attached directly to the 100 to 5000 N load cell of a 250 kN Instron testing machine (model TT-KM). The specimen was placed on a 10 cm x 10 cm x 3 cm thick flat steel plate and the specimen plus ball displacement was measured using a Hewlett Packard 24DCDT-050 displacement transducer attached directly to the ball assembly with its core extension resting on the steel plate. The force displacement curves were recorded on a fast response (<1 sec for fsd) $X-Y$ recorder with the force measured from the load cell. The amplification of the load and displacement was such that on the $X-Y$ recorder 1 cm could represent a load ranging from 0.05 to 50 N and a displacement ranging from 0.13 to 2.6 μm. With this configuration there was no need to take the machine deflection or hysteresis into account, although before it was possible to get the required stability to begin the test it was necessary to run the Instron, load cell amplifier, transducer and recorder for 8 h with the test room completely closed.

3. Results

If the elastic displacement, h(e), of the specimen plus ball followed the elastic solution, then from Hertz [5] (see also [6])

$$h(\mathrm{e}) = [(1-\nu(1)^2)/E(1) + (1-\nu(2)^2)/E(2)]^{2/3} \times [9(D(1)^{-1} - D(2)^{-1})/8]^{1/3} F^{2/3} \qquad (1)$$

where $\nu(i)$ is Poisson's ratio $E(i)$ is Young's modulus, "1" refers to the ball and "2" to the specimen, $D(1)$ is the ball diameter and $D(2)$ the diameter of curvature of the indented hole and F is the applied force. The results for the initial loading at a cross head speed of 10 μm min^{-1} are shown on a $F^{2/3}$ versus h(t) plot in Fig. 1, h(t) being the total displacement h(e) + h(p) where h(p) is the plastic displacement. The dashed line is given by Equation 1 with $D(2) = \infty$ and $E(1) = 2.11 \times 10^{11}$ Pa, $\nu(1) = 0.28$, $E(2) = 7.03 \times 10^{10}$ Pa and $\nu(2) = 0.34$, values for steel and aluminium. Except for the first point at 0.25 N (25 g) the results fit this straight line until the elastic limit is reached at a load of 4.6 ± 0.2 N (0.47 kg) and displacement of 1.02 ± 0.05 μm. On unloading from 10.3 N an $F^{2/3}$ straight line is followed, though in this case it is steeper than the initial loading curve and gave a plastic deformation $h(\mathrm{p}) = 0.22$ μm. The force was then increased in a series of loadings and unloadings to a maximum of 94 N before the results shown in Fig. 2 to a maximum of 942 N were obtained. The reloading curves followed the unloading results up to the maximum previous force, and the unloading curves followed the elastic behaviour, but with a steeper slope than for $D(2) = \infty$, consistent with a decrease in $D(2)$ with increasing plastic deformation.

These results are in agreement with the suggestion of Tabor [7] that the indented hole can, on unloading, be treated as the cap of a sphere of radius of curvature greater than that of the indenter. By rearranging Equation 1

$$D(2)^{-1} = D(1)^{-1} - 8\{(1-\nu(1)^2)/E(1) + (1-\nu(2)^2)/E(2)\}^{-2} h(\mathrm{e})^3/9F^2 \qquad (2)$$

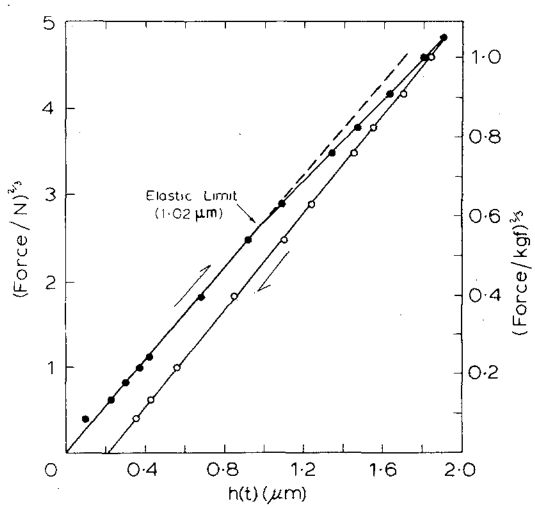

Figure 1 (Force)$^{2/3}$–displacement curve for the initial loading–unloading at 10 μm min^{-1}. The dashed line is from the Hertz solution (Equation 1) with $D(1) = 6.35$ mm and $D(2) = \infty$ while the straight line for unloading is for $D(2) = 42.4$ mm. On unloading $h(\mathrm{e}) = 1.66$ μm and $h(\mathrm{p}) = 0.22$ μm.

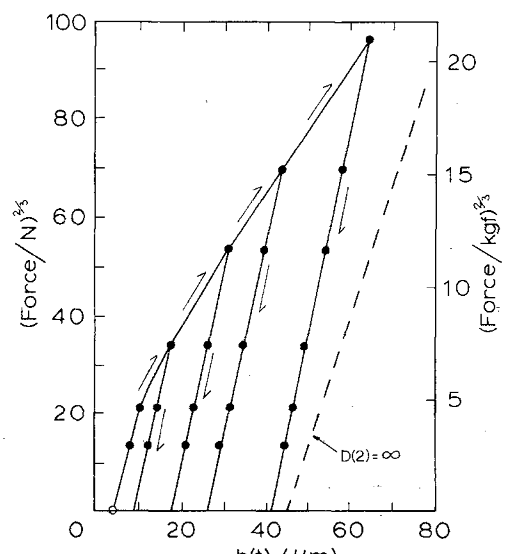

Figure 2 (Force)$^{2/3}$–displacement curve for a number of loadings and unloadings at 10 μm min^{-1}. The dashed line is for $D(2) = \infty$ while the straight lines for unloading range from $D(2) = 10.0$ to 8.77 min.

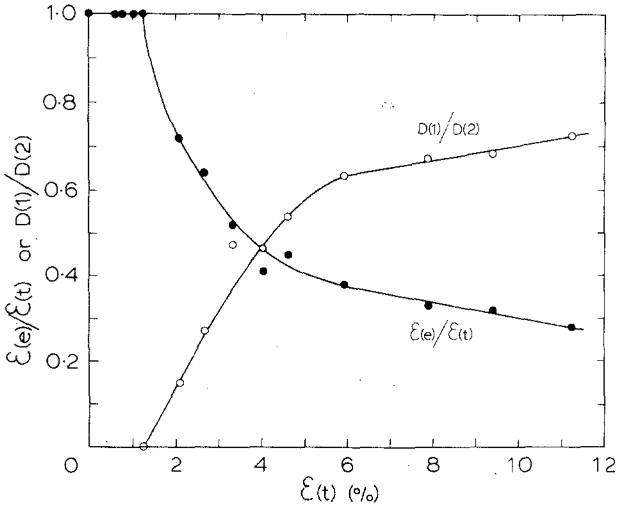

Figure 3 $D(1)/D(2)$ and $\epsilon(e)/\epsilon(t)$ versus $\epsilon(t)$ curves calculated from the unloading results; $\epsilon(e)/\epsilon(t)$ •, $D(1)/D(2)$ ○.

so that from the unloading results it is possible to determine $D(2)$. For example, on unloading from force of 10.3 N in Fig. 1, $h(e) = 1.66\,\mu m$ so that $D(2) = 42.4$ mm while from the maximum force for this test of 942 N in Fig. 2, $h(e) = 23.14\,\mu m$ and $D(2) = 8.77$ mm. The variation of $D(1)/D(2)$ with total strain is presented in Fig. 3 and has two approximately linear regions, the first with a rapid rise at the start of plastic deformation and the second, a slow increase when most of the strain is plastic.

A check of $D(2)$ can be made by measuring the diameter, $d(2)$, of the indented hole on the surface of the specimen and comparing it with the diameter calculated from

$$d(2) = \{h(p)[D(2) - h(p)]\}^{1/2}. \quad (3)$$

For the last unloading shown in Fig. 2, the measured $d(2)$ was 1.12 ± 0.02 mm while the value calculated from $D(2) = 8.77$ mm and $h(p) = 41.3$ μm was at 1.20 ± 0.05 mm just outside the estimated experimental error.

The mean stress over the area of contact between the ball and specimen [5, 6] is

$$\sigma = (8/3\sqrt{(2)}\pi)\{(1-\nu(1)^2)/E(1) + (1-\nu(2)^2)/E(2)\}^{-1}[(D(1)^{-1} - D(2)^{-1})h(e)]^{1/2}. \quad (4)$$

The dimensionless term $[(D(1)^{-1} - D(2)^{-1})h(e)]^{1/2}$ is a measure of the elastic deformation and can be used as a definition of the elastic strain, $\epsilon(e)$, while for an initially flat specimen it is reasonable to define the plastic strain as $[h(p)/D(1)]^{1/2}$ so that the total strain $\epsilon(t)$ is given by

$$\epsilon(t) = [h(p)/D(1)]^{1/2} + [(D(1)^{-1} - D(2)^{-1})h(e)]^{1/2}. \quad (5)$$

Substituting for $D(2)^{-1}$ from Equation 2 into 4 then

$$\sigma = 16\{9\pi[(1-\nu(1)^2)/E(1) + (1-\nu(2)^2)/E(2)]^2\}^{-1}(h(e)^2/F) \quad (6)$$

giving an expression for the mean stress which is independent of either the ball or indentation diameter. Therefore if, on unloading, the force displacement curve follows the $F^{2/3}$ relationship, then from the elastic displacement and the force it is possible to determine the mean stress under the ball. This mean stress has been calculated for our results for aluminium and is shown in Fig. 4. Up to a sresss of 4.7×10^8 Pa and strain of 1.27%, the results follow the elastic solution with $D(1) = \infty$. Above this strain the stress increases more slowly until from a strain of 5 to 11% the mean stress increases linearly with strain until at at total strain of 11.25% it is $11.7 \pm 0.2 \times 10^8$ Pa (115 kg mm^{-2}).

The unloading curve can also be used to estimate the Meyer stress, $\sigma(M)$, using

$$\sigma(M) = F/\pi D(2)h(p) \quad (7)$$

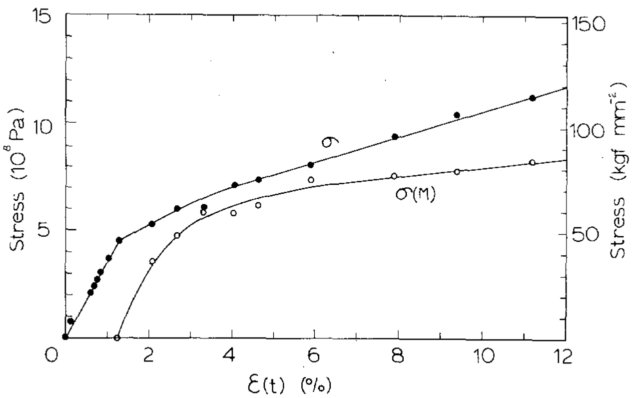

Figure 4 Stress–strain curve derived from the unloading results; • Mean stress under the ball (Equation 6), ○ Meyer stress (Equation 7).

where h(p) is the plastic displacement which is present after the load has been removed and $D(2)$ is calculated from Equation 2. The dependence of the Meyer stress on total strain is shown in Fig. 4 where it can be seen to rise rapidly at the onset of plastic deformation before rising very slowly above a strain of 6% approximately following a straight line.

The variation of $\epsilon(e)/\epsilon(t)$ with total strain, presented in Fig. 3, has two parts; the first with a rapid decrease at the start of plastic deformation and the second, a gradual linear decrease when most of the strain is plastic. The sum of $\epsilon(e)/\epsilon(t)$ plus $D(1)/D(2)$ varies from 0.87 at a strain of 2.1% to 1.00 ± 0.02 for strains 4.6% and above, indicating that

$$\epsilon(p)/\epsilon(t) \simeq D(1)/D(2), \qquad (8)$$

or by substituting Equation 5 for the strains

$$h(e)/h(p) \simeq (D(2)/D(1))\{D(2)/D(1) - 1\}. \quad (9)$$

The experimental results for $\epsilon(p)/\epsilon(t)$ and $D(1)/D(2)$ are shown in Fig. 5 and can be seen to follow approximately the straight line given by Equation 8, especially for strains above 4%. The values of $h(e)/h(p)$ given by Equation 9 for the extreme cases of $D(2)/D(1) = \infty$ and 1 are reasonable in that in the first case, where there is no plastic deformation, $h(e)/h(p) = \infty$ and in the second, where the ball indentation combination is infinitely stiff because, of the matching $h(e)/h(p)$, is zero.

A check was made of the rate-dependence of the force–displacement curves by operating the cross-head at 100 instead of 10 μm min^{-1}. The force displacement curves for the complete test at 100 μm min^{-1} agreed within ± 1% with those at 10

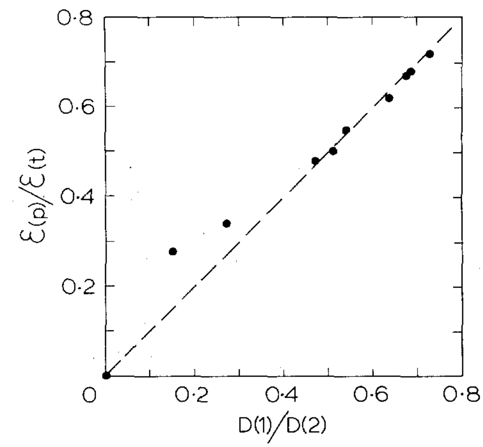

Figure 5 Variation of $\epsilon(p)/\epsilon(t)$ with $D(1)/D(2)$ determined from the unloading results. The dashed line is given by $\epsilon(p)/\epsilon(t) = D(1)/D(2)$ (Equation 8).

μm min^{-1} so that we conclude that in the range of these tests on aluminium there is no observable rate-dependence.

To enable our hardness stress–strain curve to be compared with other hardness techniques, Brinell and Vickers hardnesses were measured. For the Brinell test a load of 500 kg and a steel ball of 10 mm was used giving a Brinell hardness of 100 ± 0.5 kg mm^{-2} while the Vickers diamond pyramid with a 2.5 kg load gave a Vickers hardness of 110 kg mm^{-2}. These two hardness results are at strains well in the plastic region and can be compared with out results at $\epsilon(t) = 9\%$ with $\sigma = 107 \pm 2$ kg mm^{-2} and $\sigma(M) = 79 \pm 2$ kg mm^{-2}.

4. Conclusions

(1) The elastic loading of a spherical steel indenter into an aluminium test piece followed the classical Hertz equation. On unloading after plastic defor-

mation, $F^{2/3}$ versus the displacement followed a straight line which confirmed the relevant Hertz solution.

(2) From the elastic displacement on unloading it has been possible to determine the mean stress and the elastic strain under the ball, and the spherical diameter of the indentation. Together with the total plastic displacement these results enabled the Meyer stress and total strain to be calculated and a stress–strain diagram for hardness to be drawn.

(3) Experimentally it has been found that for aluminium the elastic and plastic strains are approximately related to the ball and indentation diameters by the equation

$$\epsilon(\mathrm{p})/\epsilon(\mathrm{t}) \simeq D(1)/D(2).$$

References

1. R. F. BUNSHAH and R. W. ARMSTRONG, in "The Science of Hardness Testing and its Research Applications", edited by J. H. Westbrook and H. Conrad (ASM, Metals Park, 1973) Chapter 26.
2. R. W. ARMSTRONG and W. H. ROBINSON, *N.Z.J. Sci.* **17** (1974) 429.
3. *Idem* submitted to *J. Mech. Phys. Solids.*
4. W. J. COUSINS, R. W. ARMSTRONG and W. H. ROBINSON, *J. Mater Sci.* **10** (1975) 1655.
5. H. R. HERTZ, "Miscellaneous Papers" (Macmillan, London 1896) Chapters 5 and 6.
6. S. P. TIMOSHENKO and J. N. GOODIER, ',Theory of Elasticity" (McGraw–Hill, New York, 1970) p. 409.
7. D. TABOR, "The Hardness of Metals" (Clarendon Press, Oxford, 1951) Chapter 6.

Received 7 January and accepted 18 February 1977.